All Fiber-Optic Neural Network Using Coupled SOA Based Ring Lasers

Martin T. Hill, *Associate Member, IEEE*, Edward E. E. Frietman, *Senior Member, IEEE*, Huig de Waardt, Giok-djan Khoe, *Fellow, IEEE,* and H. J. S. Dorren

***Abstract*—An all-optical neural network is presented that is based on coupled lasers. Each laser in the network lases at a distinct wavelength, representing one neuron. The network status is determined by the wavelength of the network's light output. Inputs to the network are in the optical power domain. The nonlinear threshold function required for neural-network operation is achieved optically by interaction between the lasers. The behavior of the coupled lasers is explained by a simple laser model developed in the paper. In particular, the winner take all (WTA) neural-network behavior of a system of many lasers is described. An experimental system is implemented using single mode fiber optic components at wavelengths near 1550 nm. A number of functions are implemented to demonstrate the practicality of the new network. The neural network is particularly robust against input wavelength variations.**

***Index Terms*—Optical computing, optical fibers, optical neural networks, semiconductor lasers.**

I. Introduction

AN AREA that has been significantly advanced by the use of optical technology is that of telecommunications. Significant research effort is being focused on directly processing the transmitted optical information in optics, rather than requiring optical to electrical conversion and electronic processing. All-optical processing may provide many benefits such as flexibility in data rates and high speed. In particular, neural-network techniques have already been applied to the tasks of routing in telecommunication networks [1], [2]. In the future, these routing tasks could be performed completely in the optical domain [3]. Another application of interest is optical processing of data packets in packet switched optical data networks.

An optical neural network that is for use in optical telecommunication systems must be compatible with the wavelengths used in telecommunications. Furthermore, it must be very robust and reliable to meet the strict bit error rate requirements, and operate at high speed.

In the past, the implementation of neural-network concepts in optics has been investigated by a number of researchers. Most research has focused on exploiting the benefits of optical interconnection between neurons via free space optics. The actual nonlinear threshold function needed for neural operation, however, is typically realized in the electronic domain [4]–[6].

There have been some attempts at obtaining fully optical neural networks using resonators and laser oscillators [7], [8]. These networks employed resonators based on photo-refractive materials and exploited gain competition between the transverse modes of the resonators.

In [9]–[11], a winner take all (WTA) neural network was demonstrated which was based on gain competition between longitudinal modes of laser diode. Each longitudinal mode had a different wavelength and the laser cavity mirror reflectivity for each mode was controlled. Here, the threshold function was in the optical domain. However, the inputs to the neural network were implemented in the optical transmission domain by inserting a liquid crystal display (LCD) in the laser feedback path. The LCD was controlled electronically. An attempt to extend this laser neural-network (LNN) concept to a system with inputs in the optical power domain was described in [12]. However, the system relied on injection locking in laser diodes, which is highly sensitive to frequency shifts between lasers. Hence, the concept was not robust enough experimentally to demonstrate any significant functions.

In this paper, systems of coupled lasers are studied. It is shown that these systems can form an optical neural network which has an optical thresholding functions, and the network inputs are in the optical power domain. Each neuron in the network is represented by a distinct wavelength. The network status being determined by the wavelength of light output λ_i, similar to the LNN in [9]. However, the system described here is not based on gain competition between lasing modes in a shared gain medium.

In particular, coupled ring lasers are considered. The ring lasers are implemented in single mode fiber-optic components at wavelengths near 1550 nm, which is compatible with telecommunication systems. Furthermore, the system could potentially be integrated in an photonic integrated circuit, reducing the laser cavity round trip time and thereby satisfying high-speed requirements.

The rest of this paper is organized as follows.

In Section II, a simplified model for a ring laser with external light injection is initially given. How two such lasers when coupled can produce an optical thresholding function is then explained. The number of lasers in the system is then increased, and it is shown that the system can function as a WTA neural network. The structure of the neural network and how weights can be implemented is also described.

Manuscript received April 11, 2001; revised January 4, 2002. This work was supported by the Netherlands Organization for Scientific Research (NWO) under the NRC Photonics Grant.

The authors are with COBRA Research Institute, Department of Electrical Engineering, Eindhoven University of Technology, 5600 MB Eindhoven, The Netherlands.

Digital Object Identifier 10.1109/TNN.2002.804222

In Section III, a neural network, as described in Section II, of four neurons and implemented with fiber-optic components is presented. A learning algorithm is used to calculate the weights necessary to implement a number of multibit functions, including the exclusive OR (XOR) function, and the WTA function. Experimental results from the neural network using the calculated weights are given.

In Sections IV and V the potential of the neural network presented here is discussed and conclusions given.

II. Principles of Operation

A. Model for a Semiconductor Ring Laser With Light Injection

A simple ring laser implemented with single mode fiber-optic components is shown in Fig. 1. The semiconductor optical amplifier (SOA) [13] acts as the laser gain medium and provides optical amplification of light traveling through it. The optical isolator allows light to travel in only one direction around the ring, thus ensuring lasing in only one direction. The wavelength filter ensures lasing at only one wavelength. The lasing wavelength is specified by the peak in the filter transmission spectrum. The coupler allows light to be coupled in and out of the ring laser.

First, we consider the operation of the solitary laser, that is, with the injected input power $P^{\text{in}} = 0$. For lasing to occur, the SOA must supply sufficient amplification or gain G, such that any losses incurred transmitting light from the SOA output back to the input are compensated for. The proportion of light transmitted from the SOA output around the loop to the SOA input is denoted by the transmittance around the loop T. T includes the transmittance of the isolator T_{iso}, the filter T_f, the coupler T_c, and losses due to component interconnections T_{con}

$$T = T_{\text{iso}} T_f T_c T_{\text{con}}. \tag{1}$$

The relation between power into the SOA P^s and power out of the SOA at the lasing wavelength P^{out} is

$$P^s = TP^{\text{out}}. \tag{2}$$

As mentioned above, G must compensate for any losses in the loop for laser oscillation to occur [14], [15]. Once lasing occurs, G is then fixed at this specific threshold gain G_{th}

$$G_{\text{th}} = 1/T. \tag{3}$$

For laser oscillation, the lasing wavelength must also satisfy the requirement that an integer number of wavelengths equals the optical length around the ring [14], [15]. The spacing $\Delta\lambda$ between adjacent wavelengths which satisfy this condition can be found to be

$$\Delta\lambda = \lambda^2/n_g L_c \tag{4}$$

where L_c is the ring length, n_g the refractive index in the ring, and λ the wavelength at which lasing occurs. In our experiments, L_c is of the order of 10 m, resulting in a very small $\Delta\lambda$. The interference filters we use have a bandwidth much larger than $\Delta\lambda$, because they are much smaller than L_c, and the minimum bandwidth they can achieve is related to their length. Thus, it is assumed that there is always a wavelength in the filter pass-band which satisfies the ring optical length wavelength requirement. Hence, this condition on wavelength is not considered further in this paper. Furthermore, it is assumed that lasing only occurs at only one wavelength in the band-pass filter, which satisfies the optical length condition mentioned above.

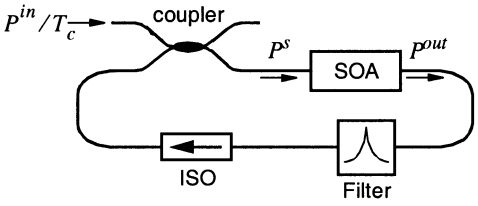

Fig. 1. Simple ring laser implemented in fiber optics, using SOA, isolator (ISO), wavelength filter, and a coupler. External power P^{in}/T_c with wavelength outside the filter pass band is injected into the laser. The transmittance through the coupler is T_c.

A neural network integrated on an optical integrated L_c circuit may be of the same order as the filter length. In this case, the choice of appropriate filter bandwidth in the optical integrated circuit design may be important [18].

Now, consider when external light via the coupler is also injected into the SOA

$$P^s = P^{\text{in}} + TP^{\text{out}}. \tag{5}$$

Note that P^{in} is the externally injected light power arriving at the SOA input after passing the coupler (see Fig. 1). Furthermore, the wavelength of P^{in} is not at the lasing wavelength of the laser and it only passes through the SOA once, as it is blocked from making a trip around the ring by the filter. However, the wavelength of P^{in} should be sufficiently close to that of the laser, so that there is not a significant difference in SOA gain between the two wavelengths [16].

In the Appendix, it is shown that given fixed operating conditions for the SOA, such as fixed injection current I, SOA parameters, and a fixed gain G_{th}, then P^s is also fixed at a unique value. This value is denoted here TP^{tot}, where P^{tot} is the value of P^{out} when $P^{\text{in}} = 0$, and it has been assumed that I is sufficiently high so that G can reach G_{th}. Increasing P^s above TP^{tot} will cause G to decrease, and lasing will no longer occur as $G < G_{\text{th}}$. Thus P^{out} (which is power at the lasing wavelength) will fall to zero.

Having P^s pegged at a unique value while maintaining sufficient gain for lasing, implies through (5) that P^{out} as a function of P^{in} is initially a straight line. The equation of the line can be found from (5) to be

$$P^{\text{out}} = P^{\text{tot}} - P^{\text{in}}/T. \tag{6}$$

After P^{out} reaches zero, which occurs when $P^{\text{in}} = P^{\text{tot}}T$, it remains at zero when P^{in} is increased further. This nonlinear optical behavior of the laser is shown in Fig. 2.

Qualitatively, the behavior shown in Fig. 2 can be explained as follows: The external photons are amplified in the SOA exactly as the photons at the lasing wavelength fed back from the SOA output. The external photons share the supply of carriers [13] used for amplification with the lasing wavelength photons. The carriers are created by the constant SOA injection current I. When the number of external photons is small, G remains at G_{th} and lasing occurs. However, each external photon takes the place

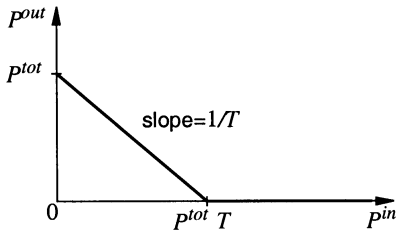

Fig. 2. Output power at the lasing wavelength P^{out} for a ring laser as a function of external light power not at the lasing wavelength injected into the ring laser P^{in}. T is the transmittance from the SOA output around the loop back to the SOA input.

of a photon at the lasing wavelength, and so P^{out} decreases linearly as a function of P^{in}. When the number of external photons is large G can no longer remain at G_{th} and is reduced, causing lasing to cease and P^{out} to fall to zero. Lasing does not occur at the wavelength of P^{in}, because the filter blocks this wavelength.

The laser model just described is quite simple and does not include the effects of spontaneous emission in the gain medium [14]. Furthermore, only the steady-state characteristics of the laser are modeled. However, the model is sufficient to describe the steady-state behavior of the neural network presented here.

B. Behavior of Two Coupled Ring Lasers

The architecture of the neural network that is considered in this paper is shown in Fig. 3 (see [17] for a discussion of neural-network architectures). The neurons (indicated by circles) are interconnected by inhibitory connections, shown by the dotted curved lines. Inputs are connected to each of the neurons by unidirectional weighted synaptic connections. The weighted synaptic connections will be discussed in Section II-C.

Fig. 4 shows the realization of the neurons and the associated inhibitory interconnections mentioned above. The set of N neurons consists of N coupled ring lasers. The PHASAR [18] (also called arrayed waveguide gratings) is an integrated optics device which provides N optical filters and additionally multiplexes the N outputs of the filters into a single output. Each filter in the PHASAR passes a different wavelength; thus, each ring laser lases at a different wavelength, denoted λ_i, corresponding to input i of the PHASAR.

The polarization controllers (PCs) in each ring laser are used to control the polarization of the light flowing back to the input of the associated SOA. The gain through the SOAs is somewhat dependent on the polarization of the input light. For each SOA in each ring laser, the polarization controllers are adjusted so that light fed back to the SOA has the polarization necessary for maximum gain.

In this section, the behavior of two coupled ring lasers is examined. The two coupled lasers are shown in Fig. 4 (with N set to two). The system of two lasers can be characterized by the following parameters:

- the power at the lasing wavelength out of the ith SOA, with no external input power and no coupling between the two lasers P_i^{tot}, $i = 1, 2$;
- the transmittance from the output of the ith SOA back to the input of the ith SOA T_{ii};

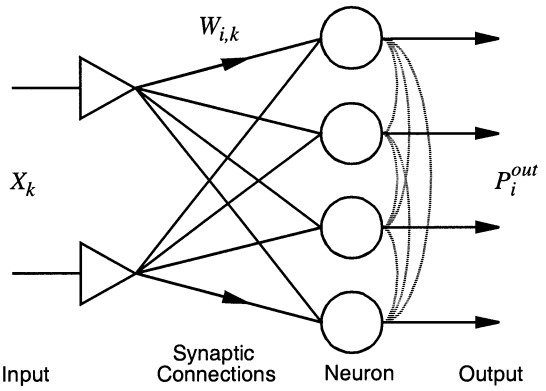

Fig. 3. Schematic drawing giving the architecture of the optical neural network considered in this paper. Neurons are indicated by circles in the figure. The neurons are interconnected in an inhibitory fashion. These inhibitory interconnections are shown by the dotted curved lines. The K network inputs X_k are connected to the N neurons via the weighted synaptic connections $W_{i,k}$. The network output consists of the optical powers P_i^{out} at the wavelength associated with each neuron.

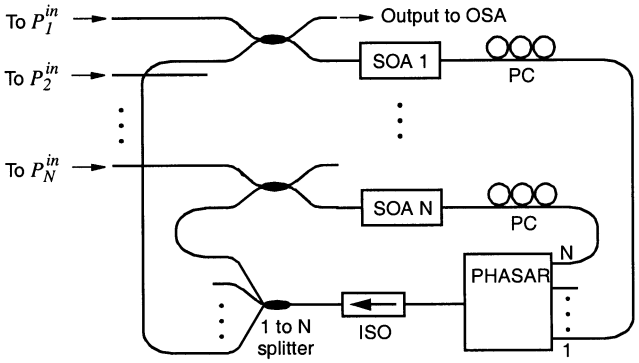

Fig. 4. Realization of the neurons shown in Fig. 3 using SOAs and fiber optics. N coupled ring lasers form the neurons. The PHASAR acts as a multichannel optical filter and multiplexer. PC—polarization controller, OSA—optical spectrum analyzer, which is used to view the neural-network output.

- the transmittance from the output of the ith SOA to the input of the jth SOA T_{ij}, $j = 3 - i$.

Note that in subsequent sections, the various optical powers will appear with a subscript indicating the laser or SOA with which they are associated.

Consider for the moment that the external inputs P_i^{in} are set to zero. The SOA injection currents are set unequal to provide asymmetry in the P_i^{tot} such that $P_1^{\text{tot}}T_{11} > P_2^{\text{tot}}T_{21}$ and $P_1^{\text{tot}}T_{12} > P_2^{\text{tot}}T_{22}$. The model of Fig. 2 predicts that laser 1 will lase under these conditions.

Furthermore, with $P_1^{\text{tot}}T_{12} > P_2^{\text{tot}}T_{22}$, laser 2 will be extinguished by the light from laser 1, because laser 1 light is also input into SOA 2. Laser 2 will output no light and have no effect on laser 1, and the system will output only light at wavelength λ_1.

As the external input P_1^{in} is increased, P_1^{out} is decreased until the light from laser 1 is insufficient to suppress laser 2. With P_1^{in} being increased further, there may be some transition region with both lasers lasing. Finally when P_1^{in} is high enough, the light from laser 2 is sufficient to suppress lasing in laser 1, and only laser 2 lases. If P_1^{in} is now reduced back to zero, the

system returns to the initial state of laser 1 lasing, and laser 2 suppressed.

In this section, the precise behavior of the system as P_1^{in} is increased is examined. It is assumed that the SOA injection currents are set unequal to provide asymmetry in the P_i^{tot} mentioned above, causing laser 1 to be the dominant laser whenever $P_1^{\text{in}} = 0$. In particular, the nature of the transition from laser 1 to laser 2 lasing depends on the relationship between T_{ii} and T_{ij}.

Three cases are considered.

1) $T_{ii} = T_{ij}$. Transmittance from SOA i output back to its own input is the same as that to SOA j.
2) $T_{ii} > T_{ij}$. Transmittance from SOA i output back to its own input is greater than that to SOA j.
3) $T_{ii} < T_{ij}$. Transmittance from SOA i output back to its own input is less than that to SOA j.

Case A—$T_{ii} = T_{ij}$: Initially, for small P_1^{in}, P_1^{out} is sufficiently large such that $P_1^{\text{out}}T_{12} > P_2^{\text{tot}}T_{22}$, and hence, lasing in laser 2 is suppressed due to the light fed from the output of laser 1 into SOA 2. As P_1^{in} increases P_1^{out} decreases with slope $1/T_{11}$, and eventually, $P_1^{\text{out}}T_{12} < P_2^{\text{tot}}T_{22}$. Thus, laser 1 is suppressed by laser 2 lasing, and P_1^{out} drops immediately to zero, as $T_{12} = T_{11}$ and $T_{22} = T_{21}$. The transition between laser 1 and laser 2 lasing is infinitely small because $T_{ii} = T_{ij}$. This behavior is summarized in Fig. 5(a).

Case B—$T_{ii} > T_{ij}$: Again, for small P_1^{in}, P_1^{out} is sufficiently large such that $P_1^{\text{out}}T_{12} > P_2^{\text{tot}}T_{22}$ and, hence, lasing in laser 2 is suppressed. As P_1^{in} is increased, $P_1^{\text{out}}T_{12}$ becomes less than $P_2^{\text{tot}}T_{22}$, and laser 2 can lase. However, initially the light from laser 2 is not sufficient to suppress laser 1 and both lase at the same time. The actual values of P_1^{out} and P_2^{out} in this transition region can be found easily by solving the following coupled linear equations:

$$P_1^{\text{out}} = (P_1^{\text{tot}} - P_1^{\text{in}}/T_{11}) - (T_{21}/T_{11})P_2^{\text{out}} \tag{7}$$

$$P_2^{\text{out}} = P_2^{\text{tot}} - (T_{12}/T_{22})P_1^{\text{out}}. \tag{8}$$

The solution to these equations are

$$P_1^{\text{out}} = \frac{(P_1^{\text{tot}} - P_1^{\text{in}}/T_{11}) - (T_{21}/T_{11})P_2^{\text{tot}}}{1 - (T_{12}/T_{11})(T_{21}/T_{22})} \tag{9}$$

$$P_2^{\text{out}} = \frac{P_2^{\text{tot}} - (T_{12}/T_{22})(P_1^{\text{tot}} - P_1^{\text{in}}/T_{11})}{1 - (T_{12}/T_{11})(T_{21}/T_{22})}. \tag{10}$$

When P_1^{in} is further increased such that $P_1^{\text{tot}}T_{21} > (P_1^{\text{tot}} - P_1^{\text{in}}/T_{11})T_{11}$, then laser 1 is completely suppressed, and laser 2 lases with output power P_2^{tot}. The behavior for this case is summarized in Fig. 5(b).

Case C—$T_{ii} < T_{ij}$: Initially, laser 1 lases. As P_1^{in} is increased, P_1^{out} decreases linearly, until $P_1^{\text{out}}T_{12} < P_2^{\text{tot}}T_{22}$. At this point, laser 2 starts to lase. In fact, P_2^{out} rapidly builds up to P_2^{tot} and suppresses lasing in laser 1 because $T_{22} < T_{12}$. An explanation for this rapid change can be found in [20]. To return to laser 1, lasing P_1^{in} must be decreased such that $(P_1^{\text{tot}} - P_1^{\text{in}}/T_{11})T_{11} > P_2^{\text{tot}}T_{21}$, which is a smaller value of P_1^{in} than initially required for laser 2 to switch on. Thus, in contrast to case A and B, there is a certain amount of hysteresis in the transition from laser 1 to laser 2 lasing. Again, the behavior for this case is summarized in Fig. 5(c).

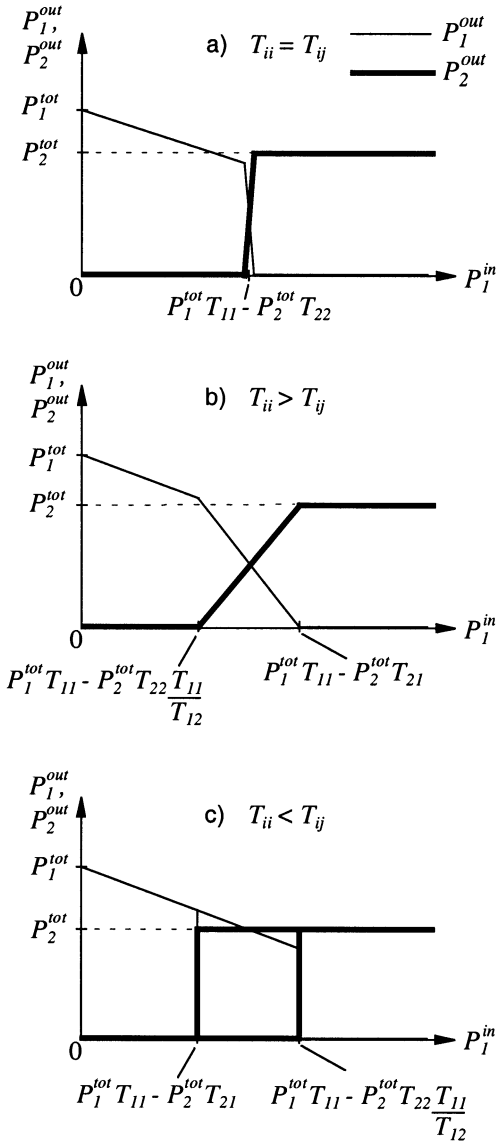

Fig. 5. Behavior of two coupled ring lasers for various levels of coupling between the two lasers. The vertical axis gives the power out of the lasers, and the horizontal axis gives the external light power injected into laser 1 P_1^{in}. The laser powers are set asymmetrically such that laser 1 dominates when $P_1^{\text{in}} = 0$. Laser 2 eventually dominates when P_1^{in} is increased sufficiently. The nature of the transition between laser 1 and laser 2 lasing depends on the coupling between the lasers.

In general, neural networks contain a nonlinear function called a threshold or sigmoid function. These functions are generally monotonically increasing functions but can also include step like functions or step functions with hysteresis in the transition region. From Fig. 5, it can be seen that the system of two coupled lasers can provide a useful sigmoid or thresholding function in the optical domain. The system can be considered as an optical neuron with wavelength λ_2 as the neuron output.

A neuron input is called an excitory input if an increase in the input causes an increase in the neuron output. Similarly, an input is inhibitory if an increase in the input causes a decrease in the output. Increases in P_1^{in} cause P_2^{out} to increase. Clearly,

P_1^{in} acts as an excitory input to neuron #2 which outputs light at wavelength λ_2. The input P_2^{in} to laser 2 can also be employed. External light input to SOA 2 will cause P_2^{tot} to decrease, and so the points where transitions occur as shown in Fig. 5 will be shifted to the right. Thus, P_2^{in} can be considered an inhibitory input to neuron #2.

Additionally, the position of the optical transition in the threshold function is controlled by the choice of initial laser powers P_1^{tot} and P_2^{tot}. These initial powers can be easily changed via the SOA injection currents.

C. N Coupled Ring Lasers to Form a WTA Network

In this section, the system of two coupled lasers is extended to N coupled lasers. However, only the case where $T_{ii} = T_{ij}$ is considered. This choice of laser coupling is particularly simple to implement. As shown in Fig. 4, a one to N splitter is all that is required to evenly distribute the output of one laser to its input and the inputs of all other lasers. Furthermore, the system forms a WTA neural network, in which only one laser can be lasing for a given set of inputs.

It is, of course, possible to form other sorts of networks besides WTA using a set of N coupled ring lasers. For example, each laser may only be coupled to nearby lasers. However, these networks are more complex to analyze, as multiple lasers may be lasing. Furthermore, there may be hysteresis in the system, even if $T_{ii} > T_{ij}$.

The neural network is required to produce an output based on the optical power in K inputs X_k, where X_k, $k \in 1, 2, \ldots, K$ gives the numerical value of the optical power in the kth input. As shown in Fig. 3, each of the K inputs are connected via a weighted synaptic connection to each of the inputs of the N neurons. The weight values are denoted $W_{i,k}$, with the k and i subscripts representing the input and laser/neuron number, respectively. That is each laser input P_i^{in} is given by the following:

$$P_i^{\text{in}} = \sum_{k=1}^{K} W_{i,k} X_k. \tag{11}$$

Fig. 6 shows a single mode fiber optic implementation of the weighted synaptic input connections for $N = 4$ and $K = 2$. The implementation requires only "1 to N" and "1 to K" splitters and variable attenuators. The variable attenuators can be adjusted to give the desired $W_{i,k}$. An alternative implementation could employ free space optics to construct a free-space optical matrix vector multiplier [19].

Using the input connection scheme described above, the maximum output for the ith laser given a particular set of inputs and assuming all other lasers are off is

$$P_i^{\text{tot}} - P_i^{\text{in}} T_{ii}. \tag{12}$$

In Section II-B, it was explained that for a system of two lasers, the laser with maximum $P_i^{\text{out}} T_{ii}$ will suppress lasing in the other laser. A similar argument holds for the system of N lasers, since the output of one laser effects all lasers equally. The laser which ends up lasing and suppresses lasing in all the other lasers will have the highest value of (13) of all the lasers, furthermore, its output power will be given by (12)

$$(P_i^{\text{tot}} - P_i^{\text{in}} T_{ii}) T_{ii}. \tag{13}$$

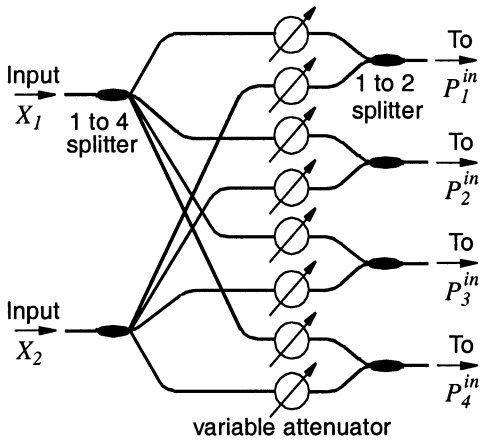

Fig. 6. Fiber optic implementation of input synaptic connections for a two-input four-laser system. The implementation uses fiber optic splitters (couplers) and variable attenuators.

Note that the weights $W_{i,k}$ defined above are actually negative weights, as they inhibit the lasing action in the laser/neuron with which they are associated. Obtaining simultaneously both positive and negative weights is a common issue in optical neural networks [21]–[23]. To enhance a particular laser and achieve a positive weight in the network presented here, the negative weights to the other lasers can be increased. Furthermore, the use of different P_i^{tot} acts effectively as an extra bias input, ensuring the correct laser lases when for example all the inputs are zero. A bias input in optical WTA networks was employed successfully in [9]. In the particular network reported here, the bias input is implemented very efficiently as the P_i^{tot} can be changed by simply varying the injected current I for each SOA.

III. Experiment

A number of experiments were performed to verify the concepts developed in Section II and demonstrate that a small WTA optical neural network could be easily made. The experiments used standard single-mode fiber-optic components, operating at wavelengths near 1550 nm.

The SOAs were supplied packaged and with fiber pigtails attached. The SOAs employed a strained bulk active region and were manufactured by JDS-Uniphase. The SOA residual facet reflectivities were less than 10^{-4} and sufficiently small so that they could be ignored. Furthermore, the maximum gain required of the SOAs in the experiments was low: less than 20 (13 dB). Hence, amplified spontaneous emission was only a small fraction of the SOA output power when they operated in the lasers. Therefore, the assumptions used in the Appendix to derive the simplified laser model used in Section II were satisfied.

A. Two Coupled Ring Lasers

For most of the experiments the setup of Fig. 4 was employed (with $N = 4$). To demonstrate the thresholding function of two lasers with approximately $T_{ii} = T_{ij}$, the setup of Fig. 4 was employed, but with only lasers 1 and 2 switched on. The SOA injection currents were set asymmetrically to give $P_1^{\text{tot}} T_{11} > P_2^{\text{tot}} T_{21}$ and thus make laser 1 dominant whenever $P_1^{\text{in}} = 0$, as described in Section II-B. The injection currents for SOA 1 and 2 were 132 and 150 mA, respectively, and with

these currents $P_1^{\text{tot}} = 161$ mW, and $P_2^{\text{tot}} = 0.73$ mW. Note that the precise relation between P_i^{tot} and the current of the specific SOA depends on the specific SOA characteristics, lasing wavelength, and losses around the ring.

External light of 1550.92 nm wavelength was injected into laser 1 via the coupler at the input of SOA 1. The injected light power P_1^{in} was varied from 0 to 0.32 mW. The values of P_1^{out} and P_2^{out} as a function of the injected light power are shown in Fig. 7.

As can be seen, a threshold function is achieved. However, the transition between laser 1 lasing and laser 2 lasing is not infinitely small as mentioned in Section II. The finite transition region is primarily due to the dependence of gain through the SOA on the polarization of the input light [24]. The polarization dependence means the gain seen by light injected into the laser is less than that seen by the light at the lasing wavelength. The polarization controller was used to obtain the maximum SOA gain for the light at the lasing wavelength and not for injected light from other sources. Furthermore, the addition of spontaneous emission further increases the transition region and causes rounding in the corners of the P_1^{out} and P_2^{out} plots.

To obtain a smaller transition between the laser 1 and laser 2 lasing, the polarization of light in the system needs to be well controlled. This control could be obtained via the use of polarization maintaining optical fibers. Alternatively, SOAs whose gain has very low polarization dependence could be used.

A second experiment was performed, with a setup similar to the one used above, to demonstrate that a threshold function with hysteresis can also be achieved. To achieve $T_{ii} < T_{ij}$, the PHASAR was replaced by a discrete Fabry–Perot filter in each ring laser. Furthermore, the one to four splitter was replaced by a fiber coupler with an unequal splitting ratio (60/40) for the two arms. The arm which carried the higher optical power out of SOA 1 was directed to the input of SOA 2. Similarly, the arm with higher optical power from SOA 2 was directed to SOA 1. In this manner, a $T_{ii} < T_{ij}$ was achieved.

The injection currents for SOA 1 and 2 were 125 mA and 120 mA, respectively. With these currents, $P_1^{\text{tot}} = 3.5$ mW and $P_2^{\text{tot}} = 2.1$ mW, which made laser 1 dominant when $P_1^{\text{in}} = 0$.

Again, a varying amount of light was injected into SOA 1. The resulting threshold function is shown in Fig. 8. The hysteresis in the transition can be clearly seen.

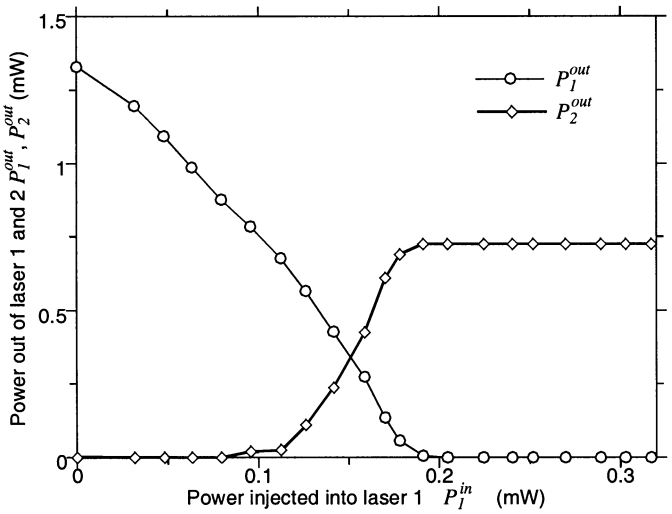

Fig. 7. Experimental results showing threshold like function produced by two coupled lasers when an increasing amount of light is injected into the dominant laser, for the case $T_{ii} = T_{ij}$.

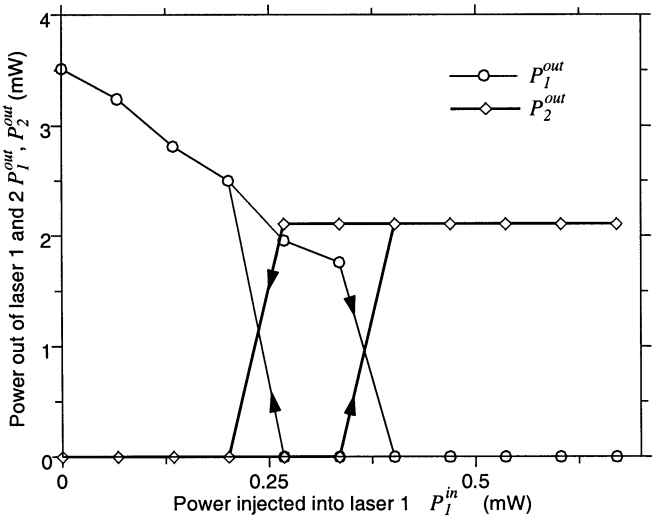

Fig. 8. Experimental results showing threshold like function which now has hysteresis in the transition from one laser to the other lasing. In particular this is for the case $T_{ii} < T_{ij}$.

B. Network of Four Coupled Ring Lasers

A network of four coupled ring lasers, as shown in Fig. 4, was constructed, along with a fiber optic network to implement the weighted synaptic connections (as shown in Fig. 6) for two optical inputs. Note that the PHASAR employed provided eight filters. The four filters with the lowest transmission loss were selected for use. With the four selected filters, the lasing wavelengths of lasers 1, 2, 3, and 4 were 1515, 1516.6, 1518.1, and 1521.3 nm, respectively.

The input weights were programmed to perform two functions of two binary optical inputs. First, a function to select the laser corresponding to the 2-bit binary input, the WTA function [9]. Second, the XOR function of the 2-bit binary input was performed. Note that a binary 1 represents an optical power of 20 mW at the input, while a binary 0 represents 0 mW.

The weights $W_{i,k}$ were calculated by a computer program using a stochastic learning algorithm identical to the one presented in [10]. The program implemented a model of the real network which used values of T_{ii} obtained from measurements of the setup. The program modeled the way the real network operated, as described in Section II-C.

Note that the learning algorithm calculated weights for a third binary input also. This third input was always set to one, and acted as a bias input. As explained in Section II-C, this bias input is necessary to achieve correct network operation. Once the weights for the bias input were found, they were translated into the corresponding P_i^{tot} and finally into an appropriate injection current for the SOA.

When the weights $W_{i,k}$ were obtained from the program, the P_i^{in} could be calculated from (11) for the various inputs. The attenuators in the input synaptic connection network were man-

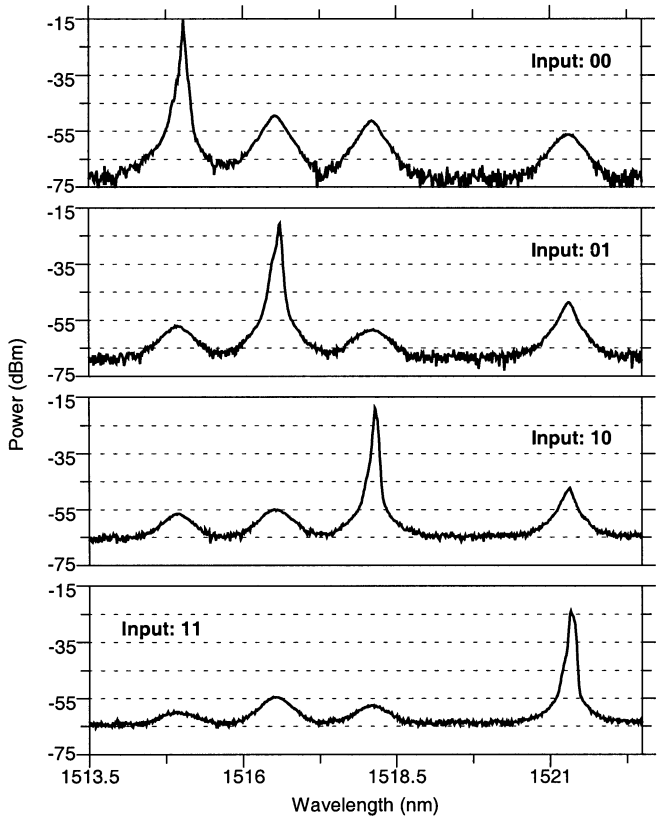

Fig. 9. Results of WTA experiment. Which laser lases is selected by the binary value of the two optical inputs. The inputs are in the optical power domain. A binary 1 represents 20 mW of optical power at the input, and a binary 0 represents 0 mW. Note the vertical scale is a logarithmic scale, and so, there is very high contrast between when a laser is on or off.

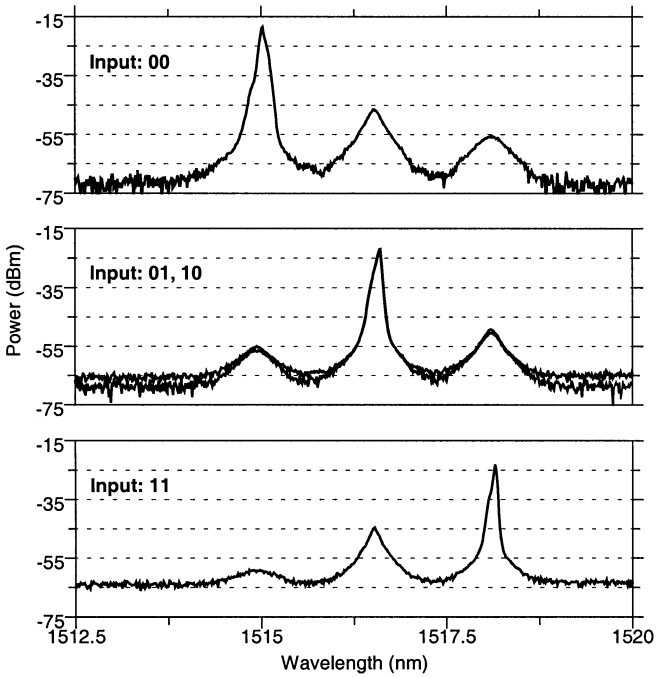

Fig. 10. Results of XOR experiment. Laser 2 performs the XOR function for the two binary inputs. Coincidentally, laser 1 is the NOR, and laser 3 is the AND function of the two inputs. Note that the results for the two input vectors 01 and 10 are plotted together on the middle graph and that the vertical scale is a logarithmic scale.

ually adjusted to give the correct P_i^{in} when the inputs were activated.

The results for the WTA and XOR networks are shown in Figs. 9 and 10, respectively. Note that the vertical scales in the figures are logarithmic scales. As can be seen from the figures, the WTA and XOR functions were successfully implemented. Furthermore, the difference in light output of a laser between when it is lasing or not is large, the contrast ratio being more than 100 : 1. Thus, there was very high contrast between the different output states of the network. Also the network was relatively insensitive to the wavelength of the inputs. Nominally, the input wavelengths were 1550.9 nm for one input bit and 1548 nm for the other input bit. However, for the WTA experiment, the wavelength of one of the input bits could be varied from 1510 to 1560 nm, a range of 50 nm, while maintaining correct operation. Finally, correct operation was maintained over a period of many days.

C. Recognition of 4-Bit Address

A target application of the network is in all optical processing of data packets in optical telecommunication systems. In these systems, the addresses of packets need to be recognized and routed to appropriate outputs [11]. Current demonstrations of all-optical address recognition have address lengths of approximately four bits [28]. Even if the address is larger, only a limited number of special patterns can be used [29], [30]. Furthermore, the current methods do not provide very high contrast in the output decisions. Typically, electronic thresholding is used after the address processor to clearly distinguish between patterns.

To demonstrate the ability of the network presented here to perform address recognition, a network as described above, but with only two lasers and four inputs, was trained to recognize the address 1010. The same methods that were used to obtain and set the input weights for the 2-bit input experiments described above were used for the 4-bit experiment.

In particular, laser 2 and 4 out of the four lasers were employed. Also the implementation of the input synaptic connections was similar to that shown in Fig. 6. However, now the four binary inputs entered on the right-hand side of Fig. 6 and the two connections to the laser were from the left-hand side.

The results of applying the 16 possible input vectors are shown in Fig. 11. As can be seen, only the input 1010 vector causes laser 2 to lase; for all other inputs, laser 4 lases. Furthermore, the contrast ratio in light output between when a laser is lasing or not is over 100 : 1, which is high.

IV. Discussion

Previous optical neural networks [10], [11], have suffered reliability problems due to the mechanical stability of the free space optics setup used to implement them. Environmental changes such as vibrations or temperature changes can have significant effects. The use of fiber optics avoids the free space optics alignment stability problems. The neural network described here operated correctly over a time span of many days, where ambient temperature changes of several degrees Celsius occurred.

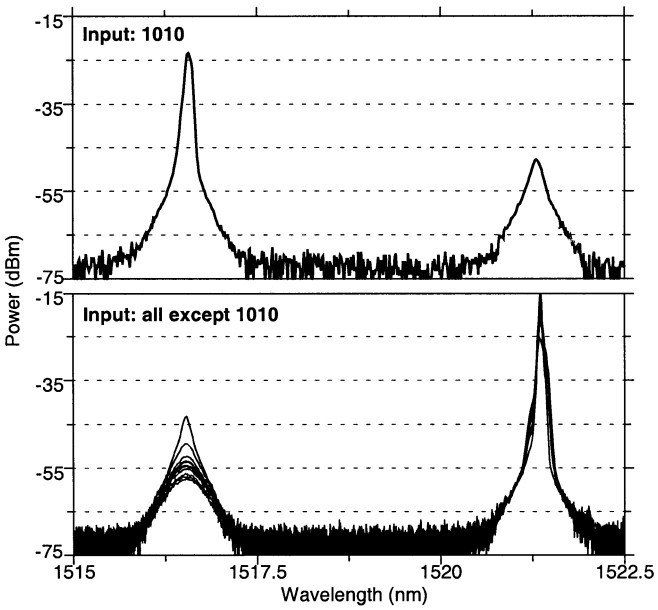

Fig. 11. Results of 4-bit address recognition experiment. The top graph shows that laser 2 lases for input vector 1010. For the other 15 possible input vectors, laser 4 lases, as shown in the bottom graph. Note the vertical scale is a logarithmic scale.

The network was also robust against variations in input wavelength. This robustness was because the interaction between the lasers themselves and between lasers and the inputs involved light which was not at the lasing wavelength of the receiving laser. Thus, no specific phase or frequency relationship needed to be maintained between the various light sources.

The stability, robustness, and optical inputs and outputs make the network suitable for the target application of all optical processing of telecommunication data. The network is also suitable for integration in a photonic integrated circuit. Components such as couplers, PHASAR, SOA, and waveguides can be integrated in a planar chip [14], [25], [26].

The neural network presented here will operate at speeds similar to the one discussed in [27]. In [27], the main factor determining system speed is the laser cavity round trip time. Hence, an integrated network with small laser cavities, would be able to respond to inputs on a nanosecond time scale, suitable for high-speed data transmission systems [27]. Furthermore, the system is not limited to ring lasers. Fabry–Perot lasers with frequency selective mirrors could also be employed. These lasers have been shown to possess the same nonlinear function as given in Fig. 2 [20].

However, there are some issues which need further investigation: For large WTA networks, the amount of feedback to each SOA is small, requiring large gains from the SOAs for lasing. For large networks, the input synaptic weighted connections will be complex to implement in planar of fiber optics. Finally, the learning and weight adjustment phase of the network is not performed optically, as the attenuators used were mechanically controlled.

It has been shown that optical WTA networks are capable of performing some moderately complex logic functions [11]. To demonstrate the ability of this particular network to perform large logic operations reliably, larger networks need to be constructed. These larger networks could consist of a single large WTA, cascaded WTA networks, or as mentioned earlier, some other network not having $T_{ii} = T_{ij}$.

For more complex functions, the precise relationships between lasers must be known. Also, how inputs affect each laser will differ due to wavelength and polarization dependence of gain [16], [24]. Thus, larger more complex networks will probably require that the learning procedure is performed with feedback from the actual network. This on-line learning will require some way to electrically control the input weights.

In operational telecommunication systems, the address length can be quite long, for example, internet protocol (IP) has 32-bit addresses and a 160-bit packet header. Distinguishing between two long addresses which differ by only one bit is not easy in one WTA neural network, as the threshold function presented here may not be sharp, nor the position of the transition well defined. However, it would be possible to recognize large addresses using a number of smaller connected neural networks.

The neural network presented here provides a way to implement complex logic functions in optics with high output contrast. The neural-network technique allows for programmability (particularly important for address recognition) and also allows compensation for the deviations in the laser device and interconnection specifications that often occur in manufacture.

One final consideration is the size of the neural network that may be implemented due to the filter wavelength spacing and finite SOA bandwidth. The spacing between the PHASAR filter wavelengths can be controlled in the PHASAR design [18]. For our experiment, the spacing was 1.6 nm. The SOAs employed had considerable gain over a bandwidth of more than 100 nm. Thus, reasonable sized networks of more than 60 neurons should be realizable.

V. Conclusion

In this paper, a number of interesting systems based on coupled ring lasers have been studied. In particular, it was shown that two coupled lasers could provide a useful and controllable threshold or sigmoid function. Furthermore, a system consisting a number of these lasers could be made to perform as a WTA neural network.

A simple laser model was developed and used to explain how the coupled laser systems worked. Also the threshold functions and WTA network were demonstrated experimentally. A number of 2- and 4-bit input logic functions were performed by the WTA network. The neural network was particularly robust against changes in input wavelength and environmental changes.

This work has been targeted toward telecommunication applications by implementing the networks at wavelengths near 1550 nm. If implemented in integrated optics, the neural network presented here could provide high-speed complex all optical logic functions required in telecommunication systems.

Appendix
Ring Laser Model Derivations

In this Appendix, it is shown that for a given set of SOA parameters and SOA injection current, there exists only one pos-

sible value of gain G for any particular total input power to the SOA P^s. Furthermore, G decreases with increasing P^s.

The SOA has received considerable attention in the literature. The derivations given here are based on the results given in [13], [24]. In this paper, a traveling wave (TW) SOA device is considered. That is, the ends of the SOA have antireflection coatings, and light flows through the device without any reflections at the SOA ends. The active region of the TW-SOA has width W, height d, and length L. Light is injected at the SOA input at position $z = 0$ and flows parallel to the z axis until it reaches the end of the SOA at $z = L$.

The SOA active region provides a net intensity gain per unit length at position z of $g(z)$

$$g(z) = \Gamma a(n(z) - n_0) - \alpha_{\text{int}} \tag{14}$$

where Γ is the optical confinement factor, a is the gain factor, $n(z)$ is the carrier density at position z, n_0 is the carrier density at transparency, and α_{int} accounts for intrinsic losses.

The photon density at position z is $S(z)$. $S(0)$ is related to the power injected into the SOA P^s by

$$S(0) = \frac{P^s}{WdH\nu v_g} \tag{15}$$

where h is Planck's constant, ν is the optical frequency, and v_g the group velocity.

The carrier density, photon density and SOA current I are related as follows [13]:

$$\frac{I}{qWdL} = \frac{n(z)}{\tau_{sp}} + \Gamma v_g a(n(z) - n_0)S(z) \tag{16}$$

with q being the electronic charge and τ_{sp} the carrier lifetime.

Assuming that the effects of spontaneous emission can be ignored, then $S(z)$ is given by the solution of the following differential equation:

$$\frac{dS(z)}{dz} = g(z)S(z). \tag{17}$$

Note that $S(z)$ needs to satisfy (14), (16), and (17), and is subject to the boundary condition (15).

G is the gain through the SOA, that is $S(L) = GS(0)$. In [13], [24] a relation is found between G, P^{in} and the SOA parameters, which satisfies (14)–(17). However, the further assumption of $\alpha_{\text{int}} = 0$ is required. In the derivation given below, the assumption of $\alpha_{\text{int}=0}$ is not required.

Equations (14), (16), and (17) can be combined to arrive at

$$dz = \frac{1 + C_2 S}{S(C_1 - \alpha_{\text{int}} C_2 S)}\, dS \tag{18}$$

where

$$C_1 = \frac{I\tau_{sp}\Gamma a}{qWdL} - n_0\Gamma a - \alpha_{\text{int}} \tag{19}$$

$$C_2 = \tau_{sp}\Gamma v_g a. \tag{20}$$

The left-hand side of (18) can be integrated from zero to L and the right-hand side from $S(0)$ to $GS(0)$ to obtain

$$C_1 L = \ln(G) + \frac{\alpha_{\text{int}} + C_1}{\alpha_{\text{int}}} \ln\left(\frac{C_1 - \alpha_{\text{int}} C_2 S(0)}{C_1 - \alpha_{\text{int}} C_2 G S(0)}\right). \tag{21}$$

For $G > 1$, the right-most term in (21) is a monotonically increasing function of $S(0)$ that ranges from 0 to ∞. Hence, there can only be at most one $S(0)$ [and via (15) one P^s] that satisfies (21), given a G. In a similar fashion, it can also be argued that as $S(0)$ is increased, G must be decreased to satisfy (21).

Note that these results have been obtained without making any assumptions on the carrier distribution throughout the SOA. With the assumption of constant gain (and thus constant carrier density) throughout the gain medium, then these results could be derived more easily [20].

In Fabry–Perot lasers, the optical fields travel in both directions through the gain medium, creating an approximately constant carrier density. However, in the ring lasers employed here, the unidirectional optical field is uneven throughout the gain medium. This unevenness can lead to a carrier distribution that is far from constant throughout the gain medium.

REFERENCES

[1] C. L. Giles and M. W. Goudreau, "Routing in optical multistage interconnection networks: A neural network solution," *J. Lightwave Technol.*, vol. 13, pp. 1111–1115, June 1995.

[2] C. J. Wang and P. N. Weissler, "The use of artificial neural networks for optimal message routing," *IEEE Network*, pp. 16–24, Mar. 1995.

[3] E. E. E. Frietman, M. T. Hill, and G. D. Khoe, "A Kohonen neural network controlled all-optical router system," *Int. J. Comput. Res.*, vol. 10, no. 2, pp. 251–267, 2001.

[4] N. H. Farhat, "Optoelectronic neural networks and learning machines," *IEEE Circuits Devices Mag.*, pp. 32–41, Sept. 1989.

[5] H. J. Caulfield, J. Kinser, and S. K. Rogers, "Optical neural networks," *Proc. IEEE*, vol. 77, pp. 1573–1583, Oct. 1989.

[6] S. Jutamulia and F. T. S. Yu, "Overview of hybrid optical neural networks," *Opt. Laser Technol.*, vol. 28, pp. 59–72, 1996.

[7] D. Z. Anderson, "Competitive and cooperative dynamics in nonlinear optical circuits," in *An Introduction to Neural and Electronic Networks*, S. F. Zornetzer, J. L. Davis, and C. Lau, Eds. New York: Academic, 1990.

[8] L. S. Lee, H. M. Stoll, and M. C. Tackitt, "Continuous-time optical neural-network associative memory," *Opt. Lett.*, vol. 14, pp. 162–164, Feb. 1989.

[9] S. B. Colak, J. J. H. B. Schleipen, and C. T. H. Liedenbaum, "Neural network using longitudinal modes of an injection laser with external feedback," *IEEE Trans. Neural Networks*, vol. 7, pp. 1389–1400, Nov. 1996.

[10] E. C. Mos, J. J. H. B. Schleipen, and H. de Waardt, "Optical mode neural network by use of the nonlinear response of a laser diode to external optical feedback," *Appl. Opt.*, vol. 36, pp. 6654–6663, 1997.

[11] E. C. Mos, J. J. H. B. Schleipen, H. de Waardt, and G. D. Khoe, "Loop-mirror neural network using a fast liquid-crystal display," *Appl. Opt.*, vol. 38, pp. 4359–4368, 1999.

[12] E. C. Mos, J. J. L. Hoppenbouwers, M. T. Hill, M. W. Blum, J. J. H. B. Schleipen, and H. de Waardt, "Optical neuron by use of a laser diode with injection seeding and external optical feedback," *IEEE Trans. Neural Networks*, vol. 11, pp. 988–995, July 2000.

[13] M. J. Adams, J. V. Collins, and I. D. Henning, "Analysis of semiconductor laser optical amplifiers," *Proc. Inst. Elect. Eng.*, pt. J, vol. 132, pp. 58–63, Feb. 1985.

[14] K. Petermann, *Laser Diode Modulation and Noise*. Dordrecht, The Netherlands: Kluwer, 1991.

[15] E. T. Peng and C. B. Su, "Properties of an external-cavity traveling-wave semiconductor ring laser," *Opt. Lett.*, pp. 55–57, Jan. 1992.

[16] I. D. Henning, M. J. Adams, and J. V. Collins, "Performance predictions from a new optical amplifier model," *IEEE J. Quantum Electron.*, vol. QE-21, pp. 609–613, June 1985.

[17] P. D. Wasserman, *Neural Computing, Theory and Practice*. New York: van Nostrand Reinhold, 1989.

[18] M. K. Smit and C. van Dam, "PHASAR-based WDM-devices: Principles, design and applications," *IEEE J. Select. Topics Quantum Electron.*, vol. 2, pp. 236–250, June 1996.
[19] J. W. Goodman, A. R. Dias, and L. M. Woody, "Fully parallel, high-speed incoherent optical method for performing discrete Fourier transforms," *Opt. Lett.*, vol. 2, pp. 1–3, Jan. 1978.
[20] M. T. Hill, H. de Waardt, G. D. Khoe, and H. J. S. Dorren, "All optical flip-flop based on coupled laser diodes," *IEEE J. Quantum Electron.*, vol. 37, pp. 405–413, Mar. 2001.
[21] C.-H. Wang and B. K. Jenkins, "Subtracting incoherent optical neuron model: Analysis, experiment, and applications," *Appl. Opt.*, vol. 29, pp. 2171–2186, May 1990.
[22] W. Kawakami, H. Yoshinaga, and K. Kitayama, "Demonstration of an optical inhibitory neural network," *Opt. Lett.*, vol. 14, pp. 984–986, Sept. 1989.
[23] J. H. Hong, S. Campbell, and P. Yeh, "Optical pattern classifier with Perceptron learning," *Appl. Opt.*, vol. 29, pp. 3019–3025, July 1990.
[24] J. C. Simon, "Semiconductor laser amplifier for single mode optical fiber communications," *J. Opt. Commun.*, vol. 4, pp. 51–62, 1983.
[25] P. A. Besse, M. Bachmann, H. Melchoir, L. B. Soldano, and M. K. Smit, "Optical bandwidth and fabrication tolerances of multimode interference couplers," *J. Lightwave Technol.*, vol. 12, no. 6, pp. 1004–1009, June 1994.
[26] O. Zhuromskyy, M. Lohmeyer, N. Bahlmann, H. Dotsch, P. Hertel, and A. F. Popkov, "Analysis of polarization independent Mach–Zehnder-type integrated optical isolator," *J. Lightwave Technol.*, vol. 17, no. 7, pp. 1200–1205, July 1999.
[27] E. C. Mos, J. J. H. B. Schleipen, H. de Waardt, and G. D. Khoe, "Longitudinal mode-switching dynamics in a dual external-cavity laser diode," *IEEE J. Quantum Electron.*, vol. 36, pp. 486–495, Apr. 2000.
[28] I. Glesk, J. P. Solokoff, and P. R. Prucnal, "All-optical address recognition and self-routing in a 250 Gbit/s packet switched network," *Electron. Lett.*, vol. 30, pp. 1322–1323, 1994.
[29] D. Cotter, J. K. Lucek, M. Shabeer, K. Smith, D. C. Rogers, D. Nesset, and P. Gunning, "Self-routing of 100 Gbit/s packets using 6 bit 'keyword' address recognition," *Electron. Lett.*, vol. 31, pp. 1475–1476, 1995.
[30] N. Calabretta, Y. Liu, H. d. Waardt, M. T. Hill, G. D. Khoe, and H. J. S. Dorren, "Multiple-output all-optical header processing technique based on two-pulse correlation principle," *Electron. Lett.*, vol. 37, pp. 1238–1240, 2001.

Martin T. Hill (S'96–A'97) was born in Sydney, Australia, in 1968. He received the B.E. degree with first class honors in 1990 and the M.Eng.Sc. degree in 1992 from the University of Western Australia, Adelaide, and the Ph.D. degree in 1997 from Curtin University of Technology, Perth, Australia.

During 1990, he was a Member of the Technical Staff at QPSX Communications Pty. Ltd., and from 1993 to 1998, he worked at the Australian Telecommunications Research Institute. Since 1998, he has been working in the Department of Electrical Engineering at the Technical University of Eindhoven, Eindhoven, The Netherlands, where he is involved in research on photonic components for optical packet switching. His research interests include synchronization, semiconductor laser physics, and photonic digital logic and memory devices.

Edward E. E. Frietman (S'81–M'82–SM'02) received the Bachelor and Ph.D. degrees from Delft University of Technology, Delft, The Netherlands in 1988 and 1995, respectively.

From 1999 through 2001, he was a Visiting Senior Fellow at the Research Group Electro Optical Communication Systems of Electrical Engineering at Technical University Eindhoven, Eindhoven, the Netherlands. He is currently a Visiting Professor of Applied Sciences at Delft University of Technology and an Adjunct Professor at the College of Engineering, Computer Science and Technology at California State University, Chico. He has authored and co-authored book chapters, journal articles, short communications, and contributions to conference proceedings, co-edited a series of research monographs in parallel and distributed computing, and tutored for several years SPIE short courses on optical interconnects in computers in the United States, Europe, and the Far East.

Dr. Frietman has served in a variety of regional, national, and international capacities. He is a Senior Member of the Society for Computer Simulation (SCS).

Huig de Waardt was born in Voorburg, The Netherlands, on December 1, 1953. He received the M.Sc. and Ph.D. degrees in electrical engineering from the Delft University of Technology, Delft, The Netherlands, in 1980 and 1995, respectively.

In 1981, he joined the Department of Physics, KPN Research, Leidschendam, The Netherlands, where he was engaged into research on the performance aspects of long-wavelength semiconductor laser diodes, LEDs, and photodiodes. In 1989, he moved to the Department of Transmission, where he has been working in the fields of high bit-rate direct-detection systems, optical preamplification, wavelength division multiplexing, dispersion related system limitations, and the system application of resonant optical amplifiers. He contributed to (inter)national standardization bodies and to the EURO-COST activities 215 and 239. In October 1995, he was appointed as Associate Professor at the University of Eindhoven, Eindhoven, The Netherlands, Faculty of Electrical Engineering, in the area of high-speed trunk transmission. His current research interests are in applications of semiconductor optical amplifiers, high-speed OTDM transmission, and WDM optical networking. He was active in European research programs as ACTS BLISS, ACTS Upgrade, and ACTS APEX. At present, he coordinates the TU/e activities in the European projects IST METEOR and IST FASHION. He is Member of the program committee of the national project BTS RETINA. He (co)authored more than 60 refereed papers and conference contributions.

Giok-djan Khoe (S'71–M'71–SM'85–F'91) was born in Magelang, Indonesia, on July 22, 1946. He received the Elektrotechnisch Ingenieur degree (*cum laude*), from the Eindhoven University of Technology, Eindhoven, The Netherlands, in 1971.

From 1971 to 1972, he worked at the FOM Institute of Plasma Physics, Rijnhuizen, The Netherlands, on laser diagnostics of plasmas. In 1973, he joined the Philips Research Laboratories, and in addition, he has been a part time Professor at the Eindhoven University of Technology since 1983. He became a Full Professor at the same university in 1994 and is currently Chairman of the Department of Telecommunication Technology and Electromagnetics. Research areas pursued within his chair at the university include high-capacity optical systems, all optical signal processing, systems using optical polymer fibers, packaging and pigtailing of photonic chips, optical networking, and networks that combine radiocommunication and optical communication. His work has been devoted to single-mode fiber systems and components. He has more than 40 United States Patents and has authored and coauthored more than 100 papers, invited papers, and books.

Dr. Khoe served on many international conferences in technical committees, management committees, and advisory committees as a member or chairman. He has been involved in journal activities, such as associate editor or as member of the advisory board. In Europe, he is closely involved in Community Research Programs and Dutch national research programs as participant, evaluator, auditor, and program committee member. He is one of the founders of the Dutch COBRA University Research Institute and is one of the three recipients of the prestigious "Top Research School Photonics" grant that is awarded to COBRA in 1998 by the Netherlands Ministry of Education, Culture, and Science. In 2000, the COBRA Institute welcomed Meint Smit, a recipient of the IEEE/LEOS Engineering and Ton Koonen, a Bell Labs Fellow. These two distinguished Dutch scientists decided to join the research center in Eindhoven as full Professors. He served in the IEEE/LEOS Board of Governors as European Representative, VP, and Elected Member, has been a Member of the Executive Committee of the IEEE Benelux Section, and was the founder of the IEEE/LEOS Benelux Chapter. He was a recipient of the MOC/GRIN Award in 1997.

H. J. S. Dorren, photograph and biography not available at the time of publication.